Multiple Sclerosis and Related Disorders 37 (2020) 101426

Contents lists available at ScienceDirect

Multiple Sclerosis and Related Disorders

journal homepage: www.elsevier.com/locate/msard

Review article

Correlation between EDSS scores and cervical spinal cord atrophy at 3T MRI in multiple sclerosis: A systematic review and meta-analysis

Song Xiaodong, Li Dawei, Qiu Zhandong, Su Shengyao, Wu Yan, Wang Jingsi, Liu Zheng*, Dong Huiqing*

Department of Neurology, Xuanwu Hospital, Capital Medical University, Beijing 100053, PR China

ARTICLE INFO

Keywords:
Expanded Disability Status Scale
Cervical spinal cord atrophy
Multiple sclerosis
3.0-Tesla MRI
meta-analysis

ABSTRACT

Background: Cervical spinal cord atrophy (CSCA), which partly reflects the axonal loss in the spinal cord, is increasingly recognized as a valuable predictor of disease outcome. However, inconsistent results have been reported regarding the correlation of CSCA and clinical disability in multiple sclerosis (MS). The aim of this meta-analysis was to synthesize the available data obtained from 3.0-Tesla (3T) MRI scanners and to explore the relationship between CSCA and scores on the Expanded Disability Status Scale (EDSS).

Methods: We searched PubMed, Embase, and Web of Science for articles published from the database inception to February 1, 2019. The quality of the articles was assessed according to a quality evaluation checklist which was created based on the Strengthening the Reporting of Observational Studies in Epidemiology (STROBE) guidelines. We conducted a meta-analysis of the correlation between EDSS scores and CSCA at 3T MRI in MS.

Results: Twenty-two eligible studies involving 1933 participants were incorporated into our meta-analysis. Our results demonstrated that CSCA was negatively and moderately correlated with EDSS scores (r_s = -0.42, 95% CI: -0.51 to -0.32; $p < 0.0001$). Subgroup analyses revealed a weaker correlation in the group of relapsing-remitting multiple sclerosis (RRMS) and clinically isolated syndrome (CIS) (r_s = -0.19, 95% CI: -0.31 to -0.07; $p = 0.0029$).

Conclusions: The correlation between CSCA and EDSS scores was significant but moderate. We encourage more studies using reliable and consistent methods to explore whether CSCA is suitable as a predictor for MS progression.

1. Introduction

Multiple sclerosis (MS) is a chronic immune-mediated disease that affects the neurological function of individuals in their early life. It is crucial to monitor the clinical outcomes and responses to drug treatment at the early stage of MS. Brain atrophy is thought to be closely associated with disease deterioration in MS (Bermel and Bakshi, 2006) and has been accepted as an important endpoint for monitoring treatment response in MS-related clinical trials. However, increasing evidence has demonstrated that MRI-based quantification of cervical spinal cord atrophy (CSCA) is moderately to highly correlated with the clinical status of MS (Bernitsas et al., 2015; Kearney et al., 2014b; Schlaeger et al., 2014, 2015). In addition, it is acknowledged that brain and spinal cord atrophy progresses constantly throughout the course of the disease (Minagar et al., 2004). Therefore, CSCA could be valued as a biomarker of clinical progression in future clinical practice.

However, inconsistent results have been reported regarding the clinical correlation between CSCA and clinical status in MS (Azodi et al., 2017; Bakshi et al., 2014; Daams et al., 2014; Dupuy et al., 2016). Some studies conducted cervical spinal cord segmentation with a 1.5-Tesla (1.5T) or even a 1.0 T MRI scanner (Horsfield et al., 2010; Losseff et al., 1996). 3T scanners are demonstrated to have better sensitivity and reliability than 1.5 T scanners in measuring the brain volume and cerebral deep gray matter volume in MS (Chu et al., 2017; Lysandropoulos et al., 2016). The relatively poor spatial resolution of low-field-strength MRI hampers high-quality imaging of small structures such as spinal cord, which is probably the reason for the discrepancies in this clinicoradiological correlation across studies. To increase the signal-to-noise ratio and make the results more convincing, a growing number of researchers have adopted more advanced 3T technology in their studies (Daams et al., 2014; Oh et al., 2014; Schlaeger et al., 2014). The objectives of this systematic review and meta-analysis were to synthesize the available data obtained with 3T MRI scanners and to present pooled analyses to inform clinical practice.

* Corresponding authors.
E-mail addresses: lzwcy2003@aliyun.com (Z. Liu), shshtt@sina.com (H. Dong).

https://doi.org/10.1016/j.msard.2019.101426
Received 23 April 2019; Received in revised form 28 August 2019; Accepted 30 September 2019

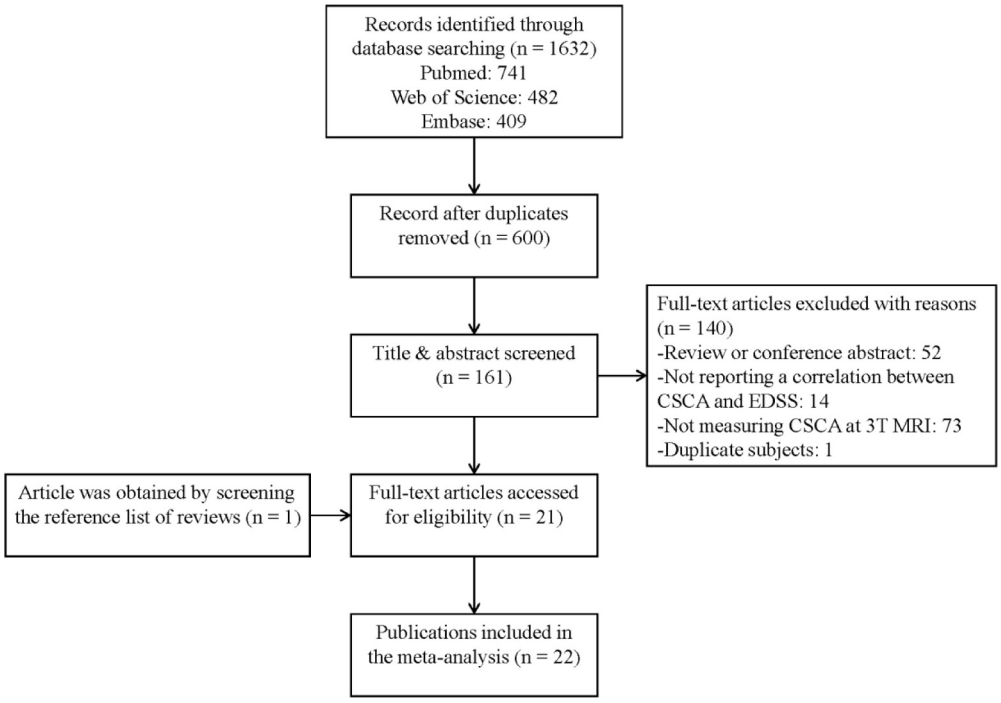

Fig. 1. Literature retrieval process.

2. Materials and methods

2.1. Data sources and searches

We performed and reported the results of this meta-analysis based on the Preferred Reporting Items for Systematic Reviews and Meta-analyses guidelines. We searched PubMed, Embase, and Web of Science for articles published from the database inception to February 1, 2019, without language restrictions. The following keywords were used in the literature search: “multiple sclerosis”, “clinically isolated syndrome”, “MS”, “CIS”, “RRMS”, “SPMS”, “PPMS”, “PMS”, “BMS”, “cord atrophy”, “cord area”, “cord cross-sectional area”, “cord volume”, “cord gray matter atrophy”, “cord gray matter area”, “cord white matter atrophy”, “cord white matter area”, “cervical”, “spinal”, and “thoracic”. We additionally scrutinized the reference lists of reviews in the retrieval results to ensure that no relevant article was omitted.

2.2. Selection criteria

Studies were eligible for our meta-analysis if they (1) enrolled people with clinically isolated syndrome (CIS), relapsing-remitting multiple sclerosis (RRMS), secondary progressive multiple sclerosis (SPMS), or primary progressive multiple sclerosis (PPMS); (2) presented 3T MRI-derived cervical spinal cord area or volume in MS patients; (3) investigated the associations between CSCA and EDSS scores; and (4) provided the regression coefficients (β), Pearson correlation coefficient (r), Spearman correlation coefficient (r_s), partial correlation coefficient (rp), or semipartial correlation (rsp) in the papers. We excluded (1) meeting abstracts, posters, case reports or reviews; (2) studies in animals or non-MS patients; (3) studies in which the correlation coefficients or regression coefficients were not available; and (4) studies based on the results from 1.0T, 1.5T or 2.0T MRI.

2.3. Data collection

Two authors (X.S. and D.L.) independently identified the titles and abstracts in the retrieval results to obtain potentially eligible studies and exclude those that were obviously irrelevant and duplicated. Then, data were extracted through reviewing the full texts of the articles fulfilling predetermined selection criteria.

The following key items were extracted on a data extraction form: authors, year of publication, countries, number of participants, basic demographics and clinical characteristics of participants, MRI sequences, spinal cord segmentation methods, software tools assistant for quantitative image analysis, and correlation coefficients. Any inconsistency about the selection of studies or data extraction was discussed in an integrative session and ultimately referred to an independent arbiter for consultation.

2.4. Study quality assessment

Another two authors (Z.L. and H.D.) independently assessed the quality of the studies. Since all studies incorporated into this meta-analysis were cross-sectional or cohort study designs, we created a quality evaluation checklist (Supplementary Table S1) based on the Strengthening the Reporting of Observational Studies in Epidemiology (STROBE) guidelines. The maximum possible score on the checklist was “20″. We regarded studies that scored “13–20″ as high quality, those that scored “7–12″ as moderate quality, and those that scored “0–7″ as low quality.

2.5. Statistical analysis

We conducted meta-analyses in R software with the "metafor" package. If values for the Spearman correlation coefficient (r_s) were not available in a particular study, the Pearson correlation coefficient (r), multiple regression coefficient (β), or coefficient of determination of simple linear regression values (R2) was used to estimate r_s according to the following formulas (1) $r_s = \frac{6}{\pi}\sin^{-1} r/2$ (Rupinski and Dunlap, 1996), (2) $r = \beta + 0.05\lambda$ (if $\beta < 0$, $\lambda = 0$; if $\beta \geq 0$, $\lambda = 1$) (Peterson and Brown, 2005), or (3) $r = \sqrt[3]{R^2}$. If the correlation coefficient in a study was reported to be not statistically significant, it was converted to zero effect. Bivariate and partial effect sizes were synthesized in one meta-analysis if (1) the synthesis included mainly bivariate effects (a small number of partial effect sizes) and (2) the summary estimates remained largely unchanged compared with the primary estimate if any single partial effect

Table 1.
Demographics and clinical characteristics of studies.

Author (year)	Country	Number	Male/ Female	Age (years)Mean ± SD (Range)	Disease Duration(years)Mean ± SD (Range)	Cross Sectional Area(mm^2)Mean ± SD (Range)	EDSSMean ± SD (Range)	CorrelationCoefficient
Cohen et al. (2012)	USA	All subjects (21) 1. CIS (1) 2. RRMS (18) 3. SPMS (1) 4. PPMS (1)	NG	40.9 ± 8 (28–55)	8.3 ± 7.5 (0.8–28)	7.51 ± 0.15 (6.04–11.42)	1.6 ± 1.6 (0–6.0)	−0.515 (Partial) $P = 0.02$
Healy et al. (2012)	USA	All subjects (34) 1. CIS (2) 2. RRMS (26) 3. PPMS (2) 4. SPMS (4)	8 M/26F	41.6 ± 8.9 (25–55)	8.37 ± 8.61 (0.2–30)	RMS (202.9 ± 22.1) PMS (161.9 ± 18.5)	1.96 (0–6.5)	−0.5 (Spearman) $P = 0.02$
Chen et al. (2013)	USA	All subjects (131)	2 M/3F		NG		NG	−0.19 (Semi-partial) $P = 0.03$
		RRMS (76)	23 M/53F	38.9 ± 10.5	NG	81.2 ± 14.6	NG	−0.01 (Semi-partial) $P = 0.95$
		PPMS (16)	8 M/8F	53.4 ± 6.7	NG	83.0 ± 19.2	NG	0.03 (Semi-partial) $P = 0.86$
		SPMS (34)	12 M/22F	51.9 ± 7.3	NG	68.7 ± 20.1	NG	−0.40 (Semi-partial) $P = 0.10$
		CIS (5)	2 M/3F	34.8 ± 9.6	NG	83.1 ± 11.1	NG	
Bakshi et al. (2014)	USA	All subjects (55) 1. CIS (4) 2. RRMS (46) 3. SPNS (4) 4. PPMS (1)	17 M/38F	41.1 ± 9	8.3 ± 7.4	2302.3 ± 350.1	1.6 ± 1.7	−0.33 (Spearman) $P = 0.015$
Daams et al. (2014)	Dutch	All subjects (196)	64 M/132F	53.38 ± 9.62 (30.67–81.11)	19.94 ± 6.89 (8.83–45.93)	72.56 ± 9.82	4.0 (1.0–8.0)	−0.296 (Partial) $P < 0.001$
		RRMS (125)	34 M/91F	50.53 ± 9.52 (30.67–70.14)	18.94 ± 6.30 (8.83–37.65)	74.47 ± 9.47	3.0 (1.0–7.5)	
		SPMS (49)	18 M/31F	56.25 ± 6.1 (45.20–72.36)	22.50 ± 8.36 (9.68–45.93)	70.46 ± 10.15	6.0 (2.5–8.0)	
		PPMS (22)	12 M/10F	62.80 ± 7.73 (49.53–81.11)	19.93 ± 6.12 (10.32–32.54)	66.39 ± 7.7	6.0 (2.5–8.0)	
Kearney et al. (2013)	England	All subjects (15)	5 M/10F	44.9 ± 12.3	NG	64.93 ± 11.79 64.11 ± 10.76 63.85 ± 11.01 67.92 ± 10.57	4 (0–6.5)	−0.745 (Spearman) −0.525 (Spearman) −0.725 (Spearman) −0.693 (Spearman)
Kearney et al. (2014)	England	All subjects (107)						−0.600 (Spearman) $P < 0.01$
		1. CIS (22)	10 M/12F	36.2 ± 9.3	0.5 ± 0.4	82.6 ± 7.3	1 (0–3)	
		2. RRMS (29)	9 M/20F	38.1 ± 9.5	6.1 ± 4.0	78.1 ± 9	2.5 (0–7)	
		3. SPMS (28)	11 M/17F	51.3 ± 9.4	20.11 ± 11.89	63.3 ± 9.8	6.5 (4–8.5)	
		4. PPMS (28)	16 M/12F	50.5 ± 9.9	10.9 ± 7.6	68.1 ± 9.7	6 (2–8)	
Liu et al. (2014)	USA	All subjects (18)	10 M/8F	47 ± 11	16 ± 11	57.4 ± 10 (whole cord)	6 (median) 4.9 (IQR)	−0.61 (Partial) $P < 0.05$
Oh et al. (2014)	USA	All subjects (133)	47 M/86F	44 ± 12	10 ± 9	77 ± 9.2 (Normalized)	3.5 (2–6)	−0.43 (Spearman) $P < 0.001$
		RMS (78)	24 M/54F	39 ± 11	7 ± 6	79.6 ± 8.5	2.5 (IQR 1.5–3.5)	−0.19 (Spearman) $P = 0.1$
		PMS (55)	23 M/32F	52 ± 8	16 ± 11	73.3 ± 8.9	6.0 (IQR 4–6.5)	−0.45 (Spearman) $P = 0.0007$

(*continued on next page*)

Table 1. (*continued*)

Author (year)	Country	Number	Male/ Female	Age (years)Mean ± SD (Range)	Disease Duration(years)Mean ± SD (Range)	Cross Sectional Area(mm^2)Mean ± SD (Range)	EDSSMean ± SD (Range)	CorrelationCoefficient
Schlager et al. (2014)	USA	All subjects (113)						−0.42 (Spearman) $P < 0.001$
		1. PMS (25)	13 M/12F	57.3 ± 10.5 58(IQR 46.6–63.6)	20.0 ± 11.4 17.5 (IQR 13.6–26.8)	69.88 ± 1.69	2.0–8.0 6 (IQR 4–6.5)	
		2. RRMS (88)	33 M/55F	48.8 ± 9.4 48.2 (IQR 42.1–55.2)	15.3 ± 8.7 13 (IQR 10.5–18.5)	77.65 ± 0.89	0–5.0 2.0 (IQR 1.5–2.5)	
Bernitsas et al. (2014)	USA	All subjects (150)	53 M/97F	41.3 ± 8.5	11.2 ± 4.5	80.2 ± 12.1	3.8 ± 2.2	−0.75 (Spearman) $P < 0.0001$
		1.RRMS(93)	26 M/57F	39.3 ± 7.9	9.3 ± 3.3	87.3 ± 8.4	2.2 ± 1.1	−0.38 (Spearman) $p = 0.0004$
		2. PMS(57)	17 M/40F	44.5 ± 8.3	14.4 ± 4.5	68.6 ± 7.4	6.3 ± 0.7	−0.40 (Spearman) $P = 0.0021$
Biberacher et al. (2015)	Germany	All subjects (239)	83 M/185F	35.8 (19–66)	3.3 ± 3.9	72.8 ± 6.6	1.0 (0–5.5)	−0.131 (Pearson) $P = 0.044$
		1.RRMS(182)	55 M/127F	36 (19–66)	4.5 ± 4.2	72.4 ± 7	1.5 (0–5.5)	
		2.CIS(85)	28 M/57F	35.2 (18–58)	0.8 ± 1.5	73.5 ± 5.8	1.0 (0–5.5)	
Kearney et al. (2015)	England	All subjects (83)						−0.45 (Multiple Regression)
		1.CIS(21)	10 M/11F	35.14 ± 8.53	0.48 ± 0.36	83.55 ± 7.42	1 (0–3)	
		2. RRMS (33)	12 M/21F	39.58 ± 9.24	6.58 ± 5.21	76.31 ± 7.72	2.5 (0–6)	
		3. SPMS (29)	12 M/17F	51.14 ± 9.35	20.21 ± 11.62,years	62.50 ± 8.63	6.5 (4–8.5)	
Liu et al. (2015)	China	RRMS (35)	8 M/27F	33.9 ± 9.2 (17–58)	3.68 ± 3.2 (0.60–15)	0.75 ± 0.09 (0.5–0.99)	3.27 ± 1.63 (0–7.5)	−0.455(Partial) −0.374 (Spearman)
Pardini et al. (2015)	England	All subjects (71)	27 M/44F	46.2 ± 10.3	15.4 ± 10	74.11 ± 11.11	4.5 (1–8.5)	−0.41 (Spearman) $P < 0.001$
		1. RRMS (44)	15 M/29F	42.2 ± 10.0	11.4 ± 8.1	77.2 ± 10.8	2 (1–7)	
		2. SPMS (27)	12 M/15F	52.4 ± 7.6	21.9 ± 9.3	69.0 ± 10	6.5 (4–8.5)	
Schlager et al. (2015)	USA	All subjects (142)				78.44		−0.48 (Spearman) $P < 0.001$
		1. RRMS(99)	36 M/63F	48.5 ± 9.5	15.2 ± 8.3	77.46	2 (median)	
		2. PMS(53)	20 M/23F	56.5 ± 10.2	20.6 ± 10.7	68.12	6 (median)	
Dupuy et al. (2016)	USA	RRMS (16)	2 M/14F	47.7 ± 7.5 (34–58)	15.0 ± 10.3 (4–35)	63.22 ± 12.86 (Lesion, $n = 10$) 75.2 ± 11.71 (No lesion, $n = 6$)	1.5 (0–2.5)	0.17 (Spearman) $P = 0.529$
Yiannakas et al. (2016)	England	All subjects (94)						−0.13 (Simple regression) −0.123 (Simple regression) −0.128 (Simple regression) −0.122 (Simple regression)
		1. CIS (21)	8 M/13F	35 ± 9	5	75.9 ± 7.9	1 (0–3.5)	
		2. RRMS (26)	9 M/17F	40 ± 10	7	68.6 ± 7.7	3 (0–6.5)	
		3. SPMS (21)	9 M/12F	51 ± 10	19	56.2 ± 10.1	7 (4.5–7.5)	
		4. PPMS (26)	15 M/11F	51 ± 9	10	61.1 ± 9.3	6 (2–7)	
Fawad et al. (2016)	Netherlands	All subjects (51) CIS (3) RRMS (43) PMS (5)	16 M/35F	40.7 ± 9.1 (21.2–55.2)	8.3 ± 7.0 (0.2–29.0)	81.6 ± 9.9 (62.1–103.6)	1.6 ± 1.7 (0–8.0)	−0.283 (Spearman) $P = 0.04$
Azodi et al. (2017)	USA	All subjects (131)						NS
		PPMS (40)	22 M/18F	54.6 ± 9	13.3 ± 9	65 ± 11	6 (4.5–6.5)	
		RRMS (74)	31 M/43F	41.6 ± 11	7.1 ± 9	73 ± 9	1.5 (1–2.5)	
		SPMS (17)	8 M/9F	54.3 ± 9	20.0 ± 6	62 ± 9	6.5 (5.5–6.5)	

(*continued on next page*)

Table 1. (*continued*)

Author (year)	Country	Number	Male/ Female	Age (years)Mean ± SD (Range)	Disease Duration(years)Mean ± SD (Range)	Cross Sectional Area(mm^2)Mean ± SD (Range)	EDSSMean ± SD (Range)	CorrelationCoefficient
Lundell et al. (2017)	Denmark	All subjects (54)						− 0.38 (Spearman) $P = 0.004$
		1. RRMS (22)	7 M/15F	40 (25–59)	9 (3–27)	73.2 (57.4–85.6)	3.5 (0–6.5)	− 0.34 (spearman) $P = 0.1$
		2. PPMS (9)	4 M/5F	40 (27–55)	3 (2–10)	78.5 (69.2–108)	4 (3.5–6.5)	− 0.34 (Spearman) $P = 0.4$
		3. SPMS (23)	13 M/10F	48 (30–62)	15 (6–43)	66.1 (47.5–86.3)	5.5 (3.5–6.5)	− 0.21 (spearman) $P = 0.34$
Biao et al. (2018)	USA	All subjects (44)						− 0.61 (Spearman)
		1. RRMS (15)	3 M/12F	49.4 ± 9.4 (32–60)	15.8 ± 7.7	NG	2.6 ± 1.3 (1–6)	
		2. PPMS (13)	5 M/8F	55.2 ± 10.2 (37–74)	15.8 ± 9.6	NG	5.7 ± 1.1 (4–6.5)	
		3. SPMS (16)	6 M/10F	59.2 ± 9.3 (45–75)	21.1 ± 10	NG	5.6 ± 1.5 (3.5–8)	

CIS, clinically isolated syndrome; RRMS, relapsing-remitting multiple sclerosis; PPMS, primary progressive multiple sclerosis; SPMS, secondary progressive multiple sclerosis; EDSS, Expanded Disability Status Scale; SD, standard error; Spearman, Spearman's rank correlation coefficient; Pearson, Pearson correlation coefficient; Simple Regression, simple regression coefficient; Multiple Regression, multiple linear regression coefficients; NG, not given; NS, not significant.

was removed. Otherwise, partial effect sizes and bivariate correlations were separately meta-analyzed since the effects of combining two types of effect sizes are not completely understood (Aloe and Thompson, 2013). Before conducting a meta-analysis, each correlation coefficient (r_s) was converted into its corresponding z value by performing Fisher's z transformation (Michael Borenstein, 2009). Then the pooled effects were transformed back to obtain the aggregated summary effect (r_s) after the meta-analysis (Michael Borenstein, 2009).

We applied the Cochran's Q test and the I^2 statistic for the assessment of heterogeneity between studies ($I^2 < 50\%$ was defined as no statistically significant heterogeneity; $I^2 > 50\%$ was defined as statistically significant heterogeneity). The selection of fixed-effects or random-effects models was depended on the significance of the I^2 index. When significant heterogeneity existed, we attempted to analyze the source of the heterogeneity by performing subgroup analyses on the basis of MS subtype, spinal cord segmentation methods, and image processing software. Sensitivity analyses were performed by deleting a single study each time to evaluate the consistency and robustness of the primary results.

We assessed publication bias by Begg's adjusted rank correlation test and Egger's regression asymmetry test. Meanwhile, a funnel plot was visually evaluated for symmetry. We concluded that no significant publication bias existed if the p-value > 0.05.

3. Result

3.1. Identification and description of studies

A total of 1632 articles were available after searching the three databases. A total of 600 articles remained after duplicate citations were excluded, and an additional 438 studies were further removed after screening the titles and abstracts. By browsing the remaining articles in full, 21 articles were found to meet our eligibility criteria. Furthermore, one additional article was obtained by scrutinizing the reference lists of the reviews. Ultimately, 22 articles with a total number of 1933 subjects were incorporated into our meta-analysis (Azodi et al., 2017; Bakshi et al., 2014; Bernitsas et al., 2015; Biberacher et al., 2015; Chen et al., 2013; Cohen et al., 2012; Daams et al., 2014; Dupuy et al., 2016; Healy et al., 2012; Kearney et al., 2015, 2014a, 2014b; Liu et al., 2014, 2015; Lundell et al., 2017; Oh et al., 2014; Pardini et al., 2015; Schlaeger et al., 2014, 2015; Xiang et al., 2019; Yiannakas et al., 2016; Yousuf et al., 2016). The literature retrieval process is shown in Fig. 1.

All studies were published between 2012 and 2019. Individual study sizes ranged from 15 to 239 participants. The mean age of the subjects ranged from 33.9 to 54.9 years, the proportion of females included in the studies ranged from 44.4% to 87.5%, and the mean disease duration ranged from 3.3 to 20.0 years. The correlation coefficient results varied across studies, with a range from 0 to −0.75. The demographics and clinical characteristics and the CSCA quantification techniques are separately summarized in Tables 1 and 2.

3.2. Methodological quality assessment outcome

According to the quality evaluation checklist (Supplementary Table S1) based on the STROBE statement, fourteen articles were evaluated to be of high quality, and eight articles were assessed to be of moderate quality. All articles obtained maximal scores on the items of background, key results, limitations, interpretation, and generalizability. No articles described how the study sample size was arrived at (Supplementary Table S2).

3.3. Overall meta-analysis

Only four studies used partial correlations to describe the linear relationship between EDSS scores and CSCA, and the pooled results

Table 2.
CSCA quantification techniques.

Study	Magnet Field Strength and Vendor	Software	MRI Sequence Used to Measure CSCA	Anatomic Location of Cord Atrophy	Method Utilized to Measure CSCA
Cohen et al. (2012)	3-T General Electric	JIM software V.5	T2-weighted fast spin-echo	SCV at C2/C3, whole cervical, whole thoracic, and whole cord volumes	Threshold based method
Healy et al. (2012)	3-T General Electric	JIM software V.3	T2-weighted fast spin-echo	SCV at C2/C3, whole cervical, whole thoracic, and whole cord volumes	Threshold based method
Chen et al. (2013)	3-T Philips	Java Integrated Science Toolkit (JIST)	magnetization transfer prepared T2*-weighted gradient echoes	SCA at C2-C5	Chen method
Bakshi et al. (2014)	3-T General Electric	Jim software V.5	T2-weighted fast spin-echo	SCA at C2/C5	Horsfield method
Daams et al. (2014)	3-T General Electric	NeuroQLab (Fraunhofer MeVis, Bremen, Germany)	3D T1-weighted sequence	SCA at C1/C2	Lukas method
Kearney et al. (2013)	3-T Philips	1. Dispunc display software package 2. JIM software V.6	T1-weighted 3D-PSIR & T1-weighted 3D-TFE	SCA at C2/C3	1 Losseff method 2 Horsfield method
Kearney et al.(2014)	3-T Philips	JIM software V.6	T1-weighted 3D-PSIR	SCA at C2/C3	Horsfield method
Liu et al. (2014)	3-T Siemens	Software developed in Matlab	T2-weighted STIR & 3D T1-weighted MP-RAGE & 3D T1-weighted GRE sequence	SCA at C1-T10 (C1-C7)	Canny method
Oh et al. (2014).	3-T Philips	Java Integrated Science Toolkit (JIST)	3D T2-weighted gradient echo	SCV at C3/C4	Chen method
Schlager et al. (2014)	3-T Siemens	JIM software V.6	T1-weighted 2D-PSIR & T2-weighted sequence	SCA at C2/C3	Horsfield method
Bernitsas et al. (2014).	3-T Siemens	Sun workstation (Sun Microsystems Inc. Mountain View, CA, USA)	3D T1-weighted MP-RAGE	SCA at C2	Losseff method
Biberacher et al. (2015)	3-T Philips & 3T Siemens	1. Amira 5.3.3, Visage Imaging, Inc. 2. FSL software	T1-weighted sequence & T2-weighted sequence	SCA at C2/C3	Losseff method
Kearney et al. (2015)	3-T Philips	JIM software V.6	T1-weighted 3D-PSIR	SCA at C2/C4	Horsfield method
liu et al. (2015)	3-T Siemens	NeuroQLab (Fraunhofe Mevis, Bremen, Germany)	T2-weighted turbo spin-echo & 3D T1-weighted MP-RAGE	SCA at C2-30 mm above	Lukas method
Pardini et al. (2015)	3-T Philips	JIM software V.6	T1-weighted sequence	SCA C2-C3	Horsfield method
Schlager et al. (2015)	3-T Siemens	JIM software V.6	T1-weighted 2D-PSIR & T2-weighted sequence	SCA at C2/C3, C3/C4, T8/T9 and T9/T10	Horsfield method
Dupuy et al. (2016)	3-T General Electric	JIM software V.7	2D T2-weighted fast spin-echo	SCA at C1/C5	Horsfield method
Yiannakas et al. (2016)	3-T Philips	1. JIM software V.6 2. Spinal Cord Toolbox (v1.0)	3D T1-weighted MP-RAGE	SCA at C2/C3,C2/C5	1 Horsfield method 2 Propseg
Fawad et al. (2016)	3-T General Electric	JIM software V.7	T2-weighted fast spin-echo	SCA at C2/5	Horsfield method
Azodi et al. (2017)	3-T Siemens	Software developed in Matlab	T1-weighted GRE sequence	SCA at C2-C3, C4-C5, T4-T9	Canny method
Lundell et al. (2017).	3-T Siemens	Software developed in Matlab	3D T1- weighted MPRAGE & FLAIR	SCA at C2	Losseff method
Biao et al. (2019)	3-T Siemens	PropSeg (Spinal Cord Toolbox v. 2.0)	3D T1-weighted MP-RAGE	ΔSCA at C1	PropSeg

3-T, 3 –Tesla; CSVA, cervical spinal cord atrophy; SCA, spinal cord area; SCV, spinal cord volume; MP-RAGE, magnetization prepared rapid acquisition gradient echo; PSIR, phased-sensitive inversion recovery; FLAIR, fluid attenuation inversion recovery; ΔSCA, the difference between mean spinal cord area value of the entire healthy control cohort and each multiple sclerosis subject spinal cord area values.

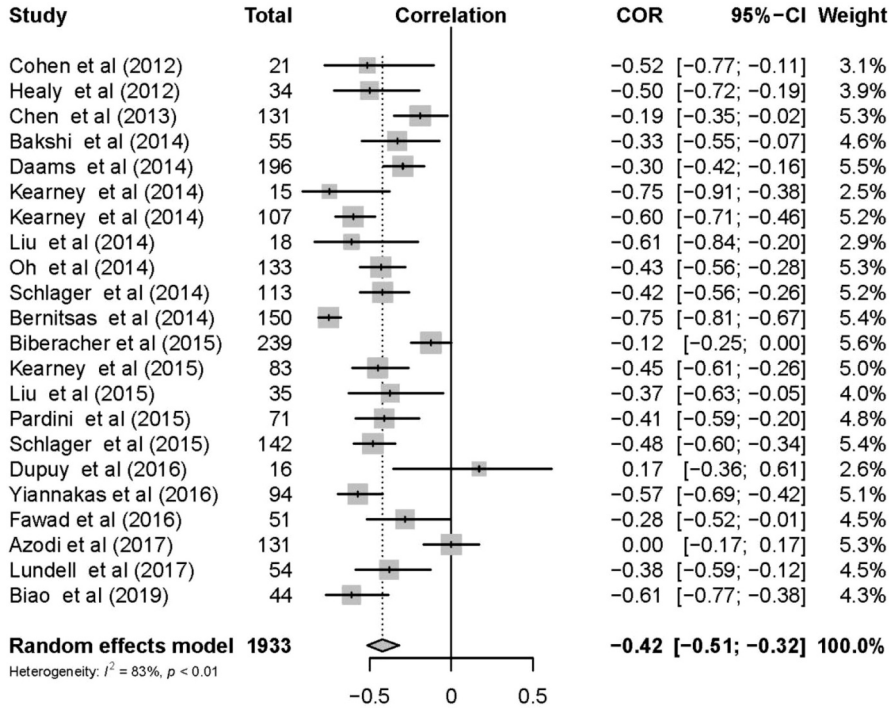

Fig. 2. Forest plots of the overall result with corresponding 95% CIs for the correlation between EDSS scores and CSCA at 3T MRI in MS patients. Summary estimates were analyzed using a random-effects model. CI: Confidence interval; COR, correlation coefficient.

remained largely unchanged when we deleted these partial effects one by one. Thus, we incorporated the four partial effects into the overall meta-analysis. Meta-analysis with a random effects model showed that EDSS scores were negatively and significantly correlated with CSCA ($r_s = -0.42$, 95% CI: −0.51 to −0.32; $p < 0.0001$; $I^2 = 83\%$). Notably, significant heterogeneity was observed across studies ($I^2 = 83\%$, $p < 0.01$; Fig. 2). According to the results of the Begg's test ($P = 0.53$) and the Egger's test ($P = 0.38$), there was no obvious evidence of publication bias and a funnel plot is shown in Fig. 3. We conducted a sensitivity analysis by omitting studies one by one, and we did not find any obviously changes in the pooled estimates compared with the primary results.

3.4. Subgroup analysis

Twenty studies enrolled participants with a mix of MS subtypes including CIS, RRMS, PPMS, and SPMS, while only two studies recruited exclusively RRMS patients. Only four studies provided additional correlation coefficients based on the different MS subtypes. Studies that contained people with CIS and RRMS were classified in the relapsing multiple sclerosis (RMS) group, and studies consisting of people with CIS, RRMS, SPMS, and PPMS were classified in the Mix group. We did not further define a progressive MS group because a limited number of SPMS and PPMS patients were available for the pooled meta-analysis. The subgroup analysis presented a weaker correlation coefficient in the RMS group ($r_s = -0.19$, 95% CI: −0.31 to −0.07; $I^2 = 44\%$) than in the Mix group ($r_s = -0.44$, 95% CI: −0.53 to −0.34; $I^2 = 72\%$). Notable heterogeneity existed in the Mix group ($I^2 = 72\%$, $p < 0.01$; Fig. 4).

Half of the studies ($n = 11$) adopted JIM software of different versions for the quantitative image analysis; the other software tools used in more than one study were JIST ($n = 2$), Spinal Cord Toolbox ($n = 2$) and NeuroQLab ($n = 3$). We divided the studies into the JIM software group and the "other software" group according to the software tools used for quantitative image analysis. The results of the pooled correlation coefficients in the JIM software group tended to be significant ($r_s = -0.46$, 95% CI: −0.53 to −0.38; $I^2 = 40\%$). Additionally, the aggregated effect of the "other software" group showed a negative correlation ($r_s = -0.43$, 95% CI: −0.57 to −0.27; $I^2 = 90\%$), and obvious heterogeneity was observed ($I^2 = 90\%$, $p < 0.01$; Fig. 5).

There was a wide variation in the spinal segmentation methods used across studies. The methods adopted in more than two studies were the Losseff method (Losseff et al., 1996) ($n = 4$) and the Horsfield method (Horsfield et al., 2010) ($n = 10$). The remaining studies used other semiautomated or automated segmentation methods including a threshold-based method (Cohen et al., 2012), the Chen method (Chen et al., 2013), the Lukas method (Lukas et al., 2004), the Canny method (Canny, 1986) and PropSeg (Yiannakas et al., 2016). We separated the studies into the Losseff method group, the Horsfield method group and the "other methods" group according to spinal cord segmentation method. Significant heterogeneity existed in the Losseff group ($r_s = -0.53$, 95% CI: −0.80 to −0.09; $I^2 = 96\%$) and the "other methods" group ($r_s = -0.40$, 95% CI: −0.52 to −0.26; $I^2 = 77\%$) compared with the Horsfield method group ($r_s = -0.45$, 95% CI: −0.54 to −0.36; $I^2 = 51\%$; Fig. 6).

Ten studies explored CSCA at C2/C3 vertebral level, and the remaining studies examined other cervical vertebral levels including C1, C2, C2 to 30 mm above, C3/C4, C2/C5, and C1-C7. We divided the studies into the C2/C3 vertebral level group and "other cervical vertebral level" group. Significant heterogeneity was shown in both groups (C2/C3 vertebral level group: $r_s = -0.43$, 95% CI: −0.56 to −0.28; $I^2 = 85\%$; "other cervical vertebral level" group: $r_s = -0.41$, 95% CI: −0.54 to −0.27; $I^2 = 83\%$; Fig. 7).

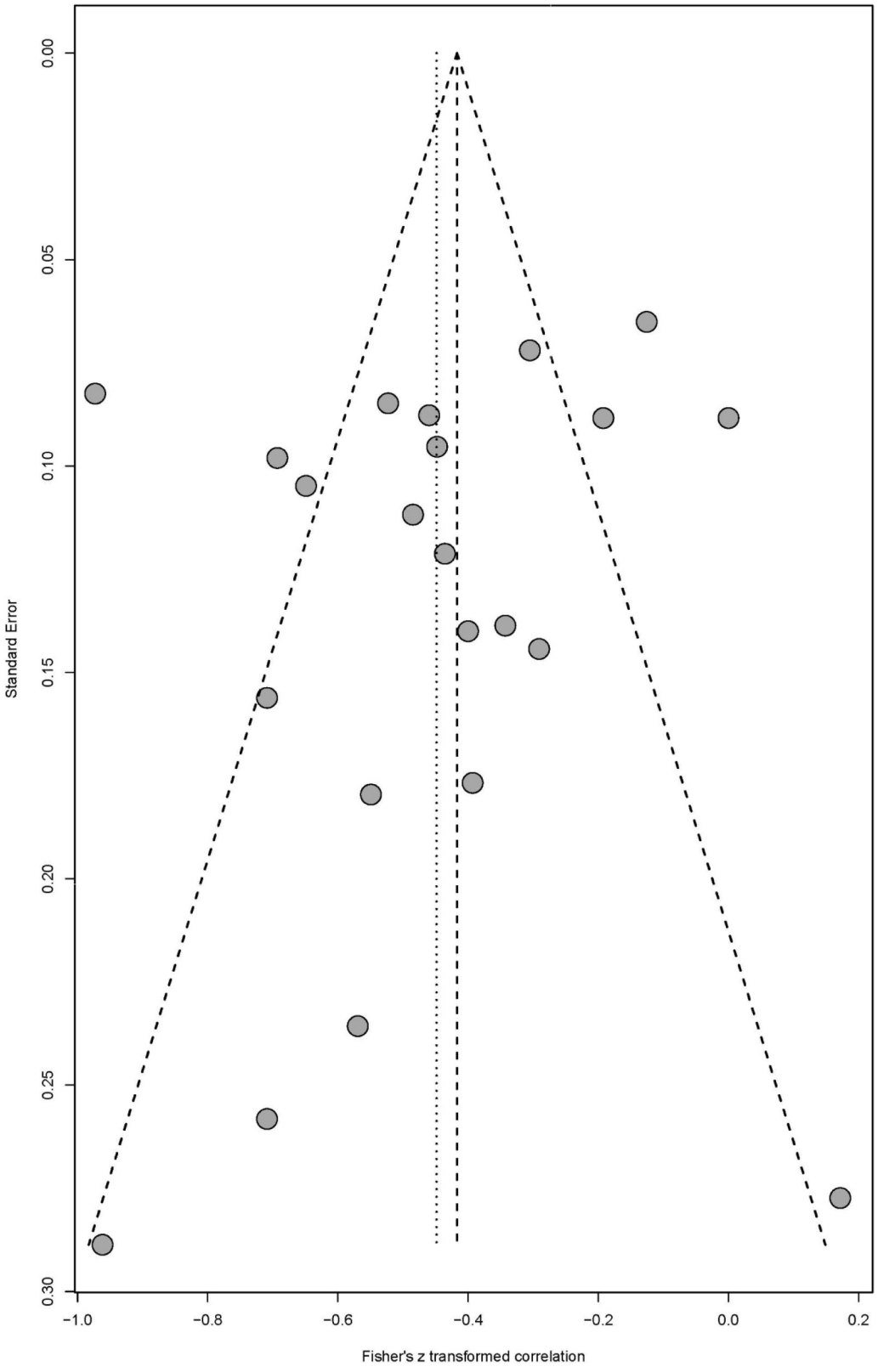

Fig. 3. Funnel graph.

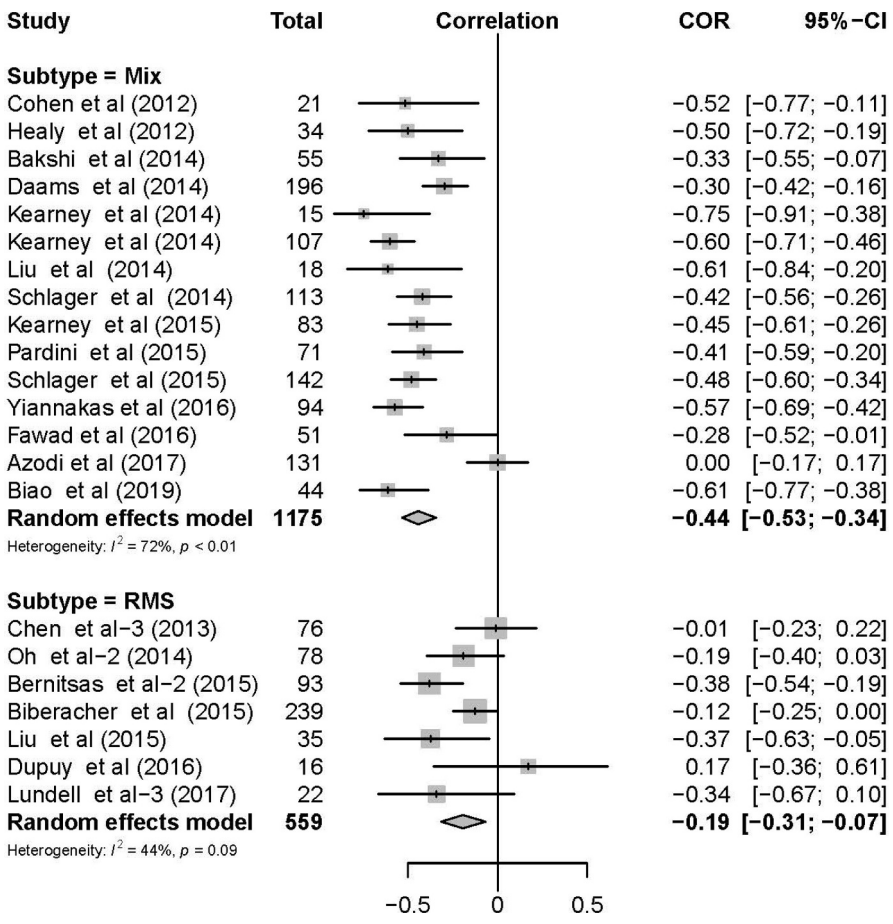

Fig. 4. Forest plots of the subgroup analysis result with corresponding 95% CIs for the correlation between EDSS scores and CSCA based on different MS subtypes. Summary estimates were analyzed using a random-effects model. Chen ea al-1, Chen ea al-2, Oh et al. − 1, Bernistas et al. − 1, Lundell et al. − 1, and Lundell et al. − 2 represented data from the progressive multiple sclerosis group. Chen ea al-3, Oh et al. − 2, Bernistas et al. − 2, and Lundell et al. − 3 represented data from the relapsing multiple sclerosis group. CI: Confidence interval; COR, correlation coefficient; Mix, Mix subgroup; RMS, relapsing multiple sclerosis subgroup.

4. Discussion

Our pooled results showed that EDSS scores had a significant association with CSCA measured by 3T MRI in people with MS. The cervical cord is a crucial crossroads between the brain and the thoracolumbar cord. Though the pathogenesis has not yet been elucidated, axonal loss in the spinal cord is mainly considered to contribute to spinal cord atrophy (DeLuca et al., 2004; Ganter et al., 1999); neuronal loss (Gilmore et al., 2009) and demyelination (Bot et al., 2004) also likely result in this pathological outcome. Axonal loss, neuronal pathology, and demyelination are recognized as the major pathological substrates of permanent functional disability in MS.

An increasing number of studies have shown cervical cord atrophy to be a predictor of clinical disability independent of brain lesion load or atrophy in MS patients (Daams et al., 2014; Schlaeger et al., 2014, 2015). Moreover, the pooled result of a recent meta-analysis has shown that the annual rate of spinal cord atrophy is 1.78% (Casserly et al., 2018), which is much higher than the rate of brain atrophy reported in a large cohort of untreated MS patients(De Stefano et al., 2010). In view of the above findings, CSCA may be a promising biomarker that will better monitor the disease progression or treatment response to novel neuroprotective agents. Our analysis provided further evidence for the clinical predictive value of CSCA.

A significant but moderate correlation between CSCA and EDSS scores was observed in our meta-analysis. The moderate correlation may be ascribed to an intrinsic defect of EDSS (Lundell et al., 2017; Noseworthy, 1994). Although the EDSS is broadly accepted as an essential MS neurological disability scale, it has limitations in evaluating disability in more severely affected MS patients, which is known as the “ceiling effect”. For example, Lundell et al. found a linear correlation between EDSS scores and CSCA reaching a plateau in more severely affected SPMS patients, and in contrast, the Multiple Sclerosis Impairment Scale still shows a good clinicoradiological correlation in those patients (Lundell et al., 2017). In addition, the EDSS is heavily weighted towards ambulatory function and is insensitive to nonambulation clinical deterioration (e.g., sexual and sphincter function) (Noseworthy, 1994). Hence, EDSS scores change little when the patient's walking ability is not severely impaired. For example, in Viola Biberacher's study, the authors ascribed the weak correlation between CSCA and disease severity to the restricted range of EDSS scores covered by their patient group (Biberacher et al., 2015). All the inherent shortcomings of EDSS mentioned above could affect the magnitude of the correlation coefficients. In addition, we should consider the inherent limitations of CSCA. A recent post mortem study found a big difference between spinal cord cross-sectional area reduction (reduction by 20%) and axonal loss (reduction by about 60%), suggesting that CSCA significantly underestimates the degree of axonal loss. Gliosis likely counteracts the spinal cord atrophy caused by nerve fiber loss (Petrova et al., 2018). Moreover, a limited number of studies have demonstrated that spinal cord gray matter atrophy is detectable in

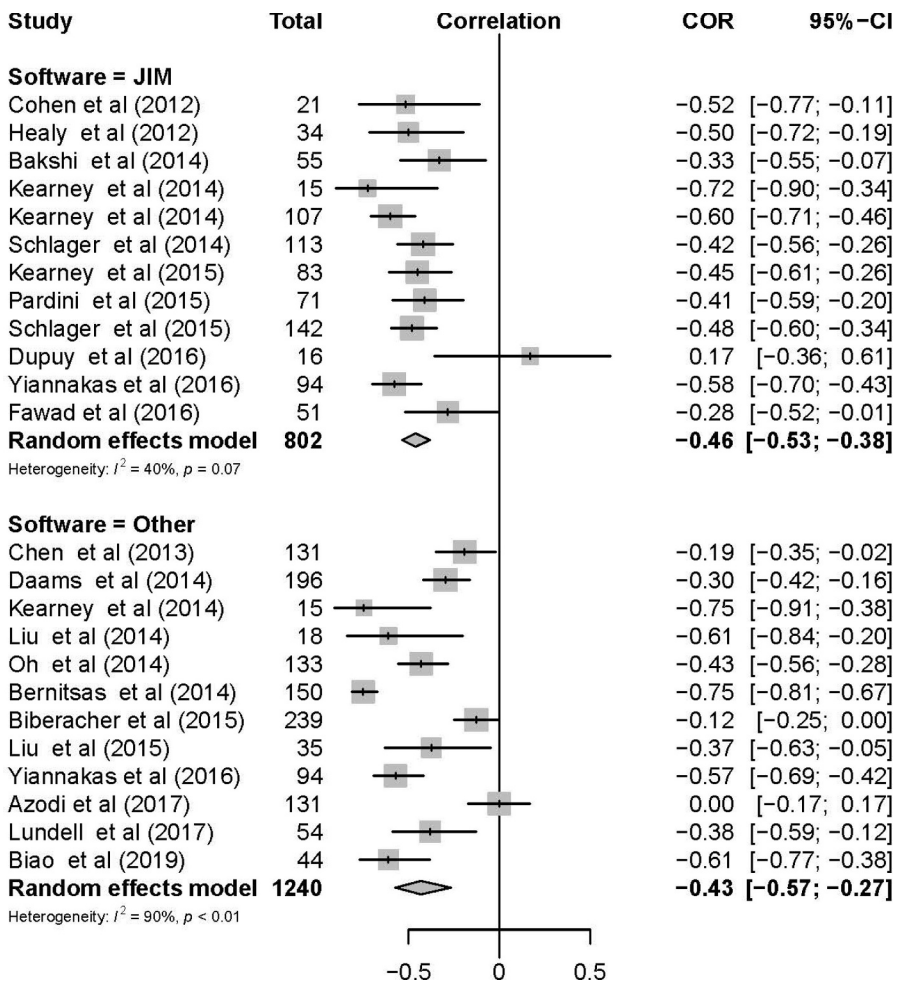

Fig. 5. Forest plots of the subgroup analysis result with corresponding 95% CIs for the correlation between EDSS scores and CSCA based on software tools assistant for quantitative image analysis. Summary estimates were analyzed using a random-effects model. CI: Confidence interval; COR, correlation coefficient; JIM, JIM software subgroup; Other, "other software" subgroup.

relapsing and progressive MS. Moreover, upper cervical cord gray matter atrophy may correlate more strongly with neurological functions than brain or cord white matter atrophy does (Schlaeger et al., 2014, 2015). Thus, these findings raise the possibility that CSCA alone cannot accurately capture the clinically relevant changes in the spinal cord. Further investigation of cord gray matter abnormalities seems worthwhile because it may improve clinical relevance.

Significant heterogeneity was shown in our meta-analysis, although Begg's adjusted rank correlation test and Egger's regression asymmetry test showed no obvious evidence of publication bias in the major outcome. To explore the source of heterogeneity, we performed a subgroup analysis based on different disease subtypes. It was suggested that the EDSS scores were negatively related to CSCA in the RMS and Mix groups. It was noteworthy that obvious heterogeneity existed in the Mix group. The reason may be that the Mix group included four different populations, which encompassed the people suffering from CIS, RRMS, SPMS, and PPMS. In addition, there appeared to be a weaker correlation in the RMS group than in the Mix group. A plausible explanation is that people with CIS or RRMS still have adequate cortical adoption reserve, which might promote rehabilitation after spinal cord or brain injury (Filippi and Rocca, 2003; Mohammed and Hollis, 2018). Adaptive changes in the cortical central nervous system allow the maintenance of normal function in the presence of irreversible axonal or neural loss (Filippi and Rocca, 2003). In people with progressive multiple sclerosis, the accumulation of tissue damage seems to exhaust this compensatory mechanism, preventing it from counteracting the functional impact of irreversible structural tissue damage (Filippi and Rocca, 2003; Filippi et al., 2013). However, there were too few studies in the RMS group, and the subgroup analysis result needs to be interpreted with caution. In addition, combining CIS and RRMS may bias the subgroup result because CIS and RRMS have some differences in clinical and radiological presentations (Miller et al., 2012). Future studies are encouraged to explore the separate associations in different subtypes of MS patients.

The heterogeneity was lower in the subgroup that applied the Horsfield method for cord segmentation than in the one that used various other segmentation methods. However, the heterogeneity was still significant in the Losseff subgroup. We speculate that the presence of too few studies using the Losseff method may have biased the subgroup results. Another plausible reason may be that the interobserver

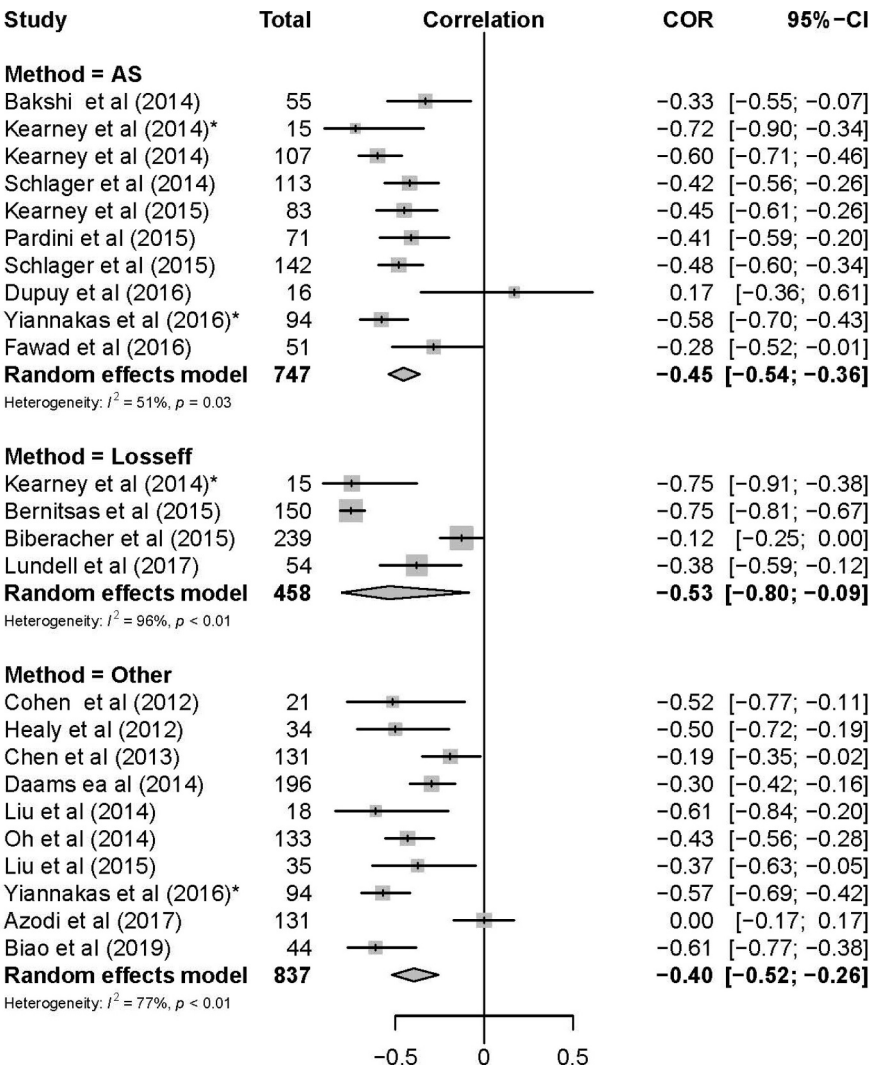

Fig. 6. Forest plots of the subgroup analysis result with corresponding 95% CIs for the correlation between EDSS scores and CSCA based on different spinal cord segmentation methods. Summary estimates were analyzed using a random-effects model. CI: Confidence interval; COR, correlation coefficient; Horsfield, Horsfield method subgroup; Losseff, Losseff method subgroup; Other, "other methods" subgroup; " * ", studies using two spinal cord segmentation methods in one research.

and intraobserver variability of measurement tend to be lower for the Horsfield method than for the Losseff method (Horsfield et al., 2010). The lower variability in the Horsfield method may have contributed to the low heterogeneity in the Horsfield method subgroup. As one might expect, lower heterogeneity was observed in the JIM software subgroup than in the "other software" subgroup, which used a variety of software tools for quantitative image analysis. Moreover, significant heterogeneity was shown in both the C2/C3 vertebral level group and the "other cervical vertebral level" group. Therefore, differences in vertebral levels used in the included studies may not have affected the heterogeneity of the meta-analysis results. In addition, to eliminate the effect of swelling on CSCA measurement, only 13 studies in our meta-analysis provided the definite exclusion criteria of the participants including no relapses and no use of corticosteroids or disease-modifying medications prior to MRI examination. Swelling of the spinal cord may be a confound to the measurement of spinal cord areas, thus resulting in heterogeneity of our meta-analysis results. Collectively, the observations mentioned above highlight the significance of adopting reliable and consistent segmentation methods and software tools as technical heterogeneity may present a challenge to comparability among clinical trials using CSCA as a clinical endpoint (Weeda et al., 2019).

Several limitations should be presented when interpreting the outcome in this meta-analysis. First, this meta-analysis is mainly based on cross-sectional data, which do not allow us to infer relatively direct relationships between CSCA and neurological functions from the results. Nevertheless, the strong correlation between CSCA changes and worsening of EDSS scores has been evidenced recently in a large cohort of people with relapse-onset MS at 6 years of follow-up (Tsagkas et al., 2018). Hence, we encourage more longitudinal studies to determine whether CSCA assessments qualify as a valuable predictor for MS progression. Second, there was obvious technical variation in the included articles, ranging from the MRI metric for CSCA quantification, the

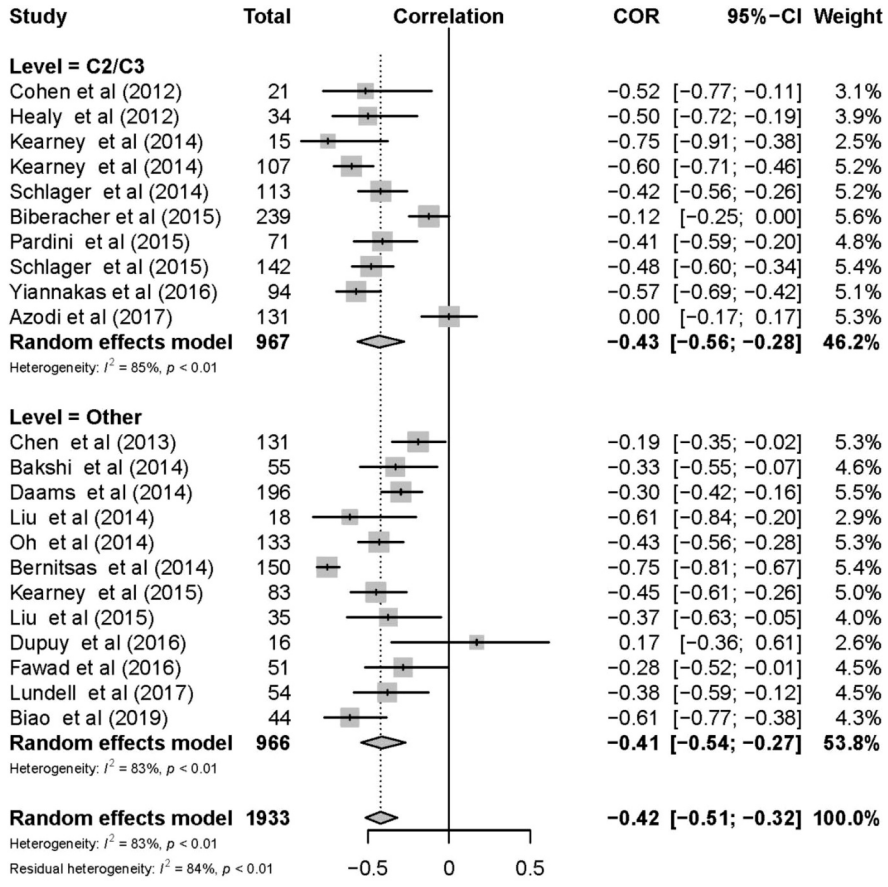

Fig. 7. Forest plots of the subgroup analysis result with corresponding 95% CIs for the correlation between EDSS scores and CSCA based on different cervical vertebral levels. Summary estimates were analyzed using a random-effects model. CI: Confidence interval; COR, correlation coefficient; C2/C3, C2/C3 cervical vertebral level subgroup; Other, "levels other cervical vertebral level" subgroup.

spinal cord segmentation method, and the image processing software. These technical heterogeneities limit the use of aggregated results as a standard reference for future trials. Third, to yield more accurate results of the correlation between CSCA and EDSS scores, we excluded studies providing 1.0T, 1.5T and 2.0T MRI-based measures of CSCA, which might have biased the results. Fourth, the subgroup analysis needs to be interpreted with caution because the results are weakened by the insufficient number of studies. Finally, the overall population included in the meta-analysis was small, and more large scale research is needed to increase the quality and credibility of the studies.

5. Conclusion

The correlation between CSCA and EDSS scores was significant but moderate. We encourage more studies using reliable and consistent methods to explore whether CSCA is suitable as a predictor for MS progression.

Declaration of Competing Interest

No conflict of interest exists in the submission of this manuscript, and the manuscript is approved by all authors for publication. All the authors listed have approved the manuscript that is enclosed.

Acknowledgments

The study was funded by the National Key R&D Program of China, Precision Medicine Program, Cohort study on nervous system diseases (2017YFC0907700), the National Science Foundation of China (grant number 81571633), Beijing Health System Clinicians Training Plan (grant number 20143054).

Supplementary materials

Supplementary material associated with this article can be found, in the online version, at doi:10.1016/j.msard.2019.101426.

References

Aloe, A.M., Thompson, C.G., 2013. The synthesis of partial effect sizes. J. Soc. Social Work Res. 4 (4), 390–405.
Azodi, S., Nair, G., Enose-Akahata, Y., Charlip, E., Vellucci, A., Cortese, I., Dwyer, J., Billioux, B.J., Thomas, C., Ohayon, J., Reich, D.S., Jacobson, S., 2017. Imaging spinal cord atrophy in progressive myelopathies: HTLV-I-associated neurological disease (HAM/TSP) and multiple sclerosis (MS). Ann. Neurol. 82 (5), 719–728.
Bakshi, R., Neema, M., Tauhid, S., Healy, B.C., Glanz, B.I., Kim, G., Miller, J., Berkowitz, J.L., Bove, R., Houtchens, M.K., Severson, C., Stankiewicz, J.M., Stazzone, L., Chitnis, T., Guttmann, C.R., Weiner, H.L., Ceccarelli, A., 2014. An expanded composite scale of MRI-defined disease severity in multiple sclerosis: MRDSS2. Neuroreport 25 (14), 1156–1161.
Bermel, R.A., Bakshi, R., 2006. The measurement and clinical relevance of brain atrophy in multiple sclerosis. Lancet Neurol. 5 (2), 158–170.
Bernitsas, E., Bao, F., Seraji-Bozorgzad, N., Chorostecki, J., Santiago, C., Tselis, A., Caon, C., Zak, I., Millis, S., Khan, O., 2015. Spinal cord atrophy in multiple sclerosis and relationship with disability across clinical phenotypes. Mult. Scler. Relat. Disord. 4 (1), 47–51.
Biberacher, V., Boucard, C.C., Schmidt, P., Engl, C., Buck, D., Berthele, A., Hoshi, M.M., Zimmer, C., Hemmer, B., Muhlau, M., 2015. Atrophy and structural variability of the upper cervical cord in early multiple sclerosis. Mult. Scler. 21 (7), 875–884 Houndmills, Basingstoke, England.
Bot, J.C., Blezer, E.L., Kamphorst, W., Lycklama, A.N.G.J., Ader, H.J., Castelijns, J.A., Ig, K.N., Bergers, E., Ravid, R., Polman, C., Barkhof, F., 2004. The spinal cord in multiple sclerosis: relationship of high-spatial-resolution quantitative MR imaging findings to histopathologic results. Radiology 233 (2), 531–540.
Canny, J., 1986. A computational approach to edge detection. IEEE Trans. Pattern Anal. Mach. Intell. 8 (6), 679–698.
Casserly, C., Seyman, E.E., Alcaide-Leon, P., Guenette, M., Lyons, C., Sankar, S., Svendrovski, A., Baral, S., Oh, J., 2018. Spinal cord atrophy in multiple sclerosis: a systematic review and meta-analysis. J. Neuroimag. Offic. J. Am. Soc. Neuroimag. 28 (6), 556–586.
Chen, M., Carass, A., Oh, J., Nair, G., Pham, D.L., Reich, D.S., Prince, J.L., 2013. Automatic magnetic resonance spinal cord segmentation with topology constraints

for variable fields of view. Neuroimage 83, 1051–1062.
Chu, R., Hurwitz, S., Tauhid, S., Bakshi, R., 2017. Automated segmentation of cerebral deep gray matter from MRI scans: effect of field strength on sensitivity and reliability. BMC Neurol. 17 (1), 172.
Cohen, A.B., Neema, M., Arora, A., Dell'oglio, E., Benedict, R.H., Tauhid, S., Goldberg-Zimring, D., Chavarro-Nieto, C., Ceccarelli, A., Klein, J.P., Stankiewicz, J.M., Houtchens, M.K., Buckle, G.J., Alsop, D.C., Guttmann, C.R., Bakshi, R., 2012. The relationships among MRI-defined spinal cord involvement, brain involvement, and disability in multiple sclerosis. J. Neuroimag. Offic. J. Am. Soc. Neuroimag. 22 (2), 122–128.
Daams, M., Weiler, F., Steenwijk, M.D., Hahn, H.K., Geurts, J.J., Vrenken, H., van Schijndel, R.A., Balk, L.J., Tewarie, P.K., Tillema, J.M., Killestein, J., Uitdehaag, B.M., Barkhof, F., 2014. Mean upper cervical cord area (MUCCA) measurement in long-standing multiple sclerosis: relation to brain findings and clinical disability. Mult. Scler. 20 (14), 1860–1865 Houndmills, Basingstoke, England.
De Stefano, N., Giorgio, A., Battaglini, M., Rovaris, M., Sormani, M.P., Barkhof, F., Korteweg, T., Enzinger, C., Fazekas, F., Calabrese, M., Dinacci, D., Tedeschi, G., Gass, A., Montalban, X., Rovira, A., Thompson, A., Comi, G., Miller, D.H., Filippi, M., 2010. Assessing brain atrophy rates in a large population of untreated multiple sclerosis subtypes. Neurology 74 (23), 1868–1876.
DeLuca, G.C., Ebers, G.C., Esiri, M.M., 2004. Axonal loss in multiple sclerosis: a pathological survey of the corticospinal and sensory tracts. Brain J. Neurol. 127 (Pt 5), 1009–1018.
Dupuy, S.L., Khalid, F., Healy, B.C., Bakshi, S., Neema, M., Tauhid, S., Bakshi, R., 2016. The effect of intramuscular interferon beta-1a on spinal cord volume in relapsing-remitting multiple sclerosis. BMC Med. Imaging 16 (1), 56.
Filippi, M., Rocca, M.A., 2003. Disturbed function and plasticity in multiple sclerosis as gleaned from functional magnetic resonance imaging. Curr. Opin. Neurol. 16 (3), 275–282.
Filippi, M., Rocca, M.A., Horsfield, M.A., Hametner, S., Geurts, J.J., Comi, G., Lassmann, H., 2013. Imaging cortical damage and dysfunction in multiple sclerosis. JAMA Neurol. 70 (5), 556–564.
Ganter, P., Prince, C., Esiri, M.M., 1999. Spinal cord axonal loss in multiple sclerosis: a post-mortem study. Neuropathol. Appl. Neurobiol. 25 (6), 459–467.
Gilmore, C.P., DeLuca, G.C., Bo, L., Owens, T., Lowe, J., Esiri, M.M., Evangelou, N., 2009. Spinal cord neuronal pathology in multiple sclerosis. Brain Pathol. 19 (4), 642–649 Zurich, Switzerland.
Healy, B.C., Arora, A., Hayden, D.L., Ceccarelli, A., Tauhid, S.S., Neema, M., Bakshi, R., 2012. Approaches to normalization of spinal cord volume: application to multiple sclerosis. J. Neuroimag. Offic. J. Am. Soc. Neuroimag. 22 (3), e12–e19.
Horsfield, M.A., Sala, S., Neema, M., Absinta, M., Bakshi, A., Sormani, M.P., Rocca, M.A., Bakshi, R., Filippi, M., 2010. Rapid semi-automatic segmentation of the spinal cord from magnetic resonance images: application in multiple sclerosis. Neuroimage 50 (2), 446–455.
Kearney, H., Schneider, T., Yiannakas, M.C., Altmann, D.R., Wheeler-Kingshott, C.A., Ciccarelli, O., Miller, D.H., 2015. Spinal cord grey matter abnormalities are associated with secondary progression and physical disability in multiple sclerosis. J. Neurol. Neurosurg. Psychiatr. 86 (6), 608–614.
Kearney, H., Yiannakas, M.C., Abdel-Aziz, K., Wheeler-Kingshott, C.A., Altmann, D.R., Ciccarelli, O., Miller, D.H., 2014a. Improved MRI quantification of spinal cord atrophy in multiple sclerosis. J. Magnet. Reson. Imag. JMRI 39 (3), 617–623.
Kearney, H., Yiannakas, M.C., Samson, R.S., Wheeler-Kingshott, C.A., Ciccarelli, O., Miller, D.H., 2014b. Investigation of magnetization transfer ratio-derived pial and subpial abnormalities in the multiple sclerosis spinal cord. Brain J. Neurol. 137 (Pt 9), 2456–2468.
Liu, W., Nair, G., Vuolo, L., Bakshi, A., Massoud, R., Reich, D.S., Jacobson, S., 2014. In vivo imaging of spinal cord atrophy in neuroinflammatory diseases. Ann. Neurol. 76 (3), 370–378.
Liu, Y., Wang, J., Daams, M., Weiler, F., Hahn, H.K., Duan, Y., Huang, J., Ren, Z., Ye, J., Dong, H., Vrenken, H., Wattjes, M.P., Shi, F.D., Li, K., Barkhof, F., 2015. Differential patterns of spinal cord and brain atrophy in NMO and MS. Neurology 84 (14), 1465–1472.
Losseff, N.A., Webb, S.L., O'Riordan, J.I., Page, R., Wang, L., Barker, G.J., Tofts, P.S., McDonald, W.I., Miller, D.H., Thompson, A.J., 1996. Spinal cord atrophy and disability in multiple sclerosis. A new reproducible and sensitive MRI method with potential to monitor disease progression. Brain J. Neurol. 119 (Pt 3), 701–708.
Lukas, C., Hahn, H.K., Bellenberg, B., Rexilius, J., Schmid, G., Schimrigk, S.K., Przuntek, H., Koster, O., Peitgen, H.O., 2004. Sensitivity and reproducibility of a new fast 3D segmentation technique for clinical MR-based brain volumetry in multiple sclerosis. Neuroradiology 46 (11), 906–915.
Lundell, H., Svolgaard, O., Dogonowski, A.M., Romme Christensen, J., Selleberg, F., Soelberg Sorensen, P., Blinkenberg, M., Siebner, H.R., Garde, E., 2017. Spinal cord atrophy in anterior-posterior direction reflects impairment in multiple sclerosis. Acta Neurol. Scand. 136 (4), 330–337.
Lysandropoulos, A.P., Absil, J., Metens, T., Mavroudakis, N., Guisset, F., Van Vlierberghe, E., Smeets, D., David, P., Maertens, A., Van Hecke, W., 2016. Quantifying brain volumes for multiple sclerosis patients follow-up in clinical practice - comparison of 1.5 and 3 Tesla magnetic resonance imaging. Brain Behav. 6 (2), e00422.
Michael Borenstein, L.V.H., Julian, P.T.Higgins, Hannah, R.Rothstein, 2009. Introduction to Meta-analysis, 1st ed. John Wiley & Sons Ltd, UK.
Miller, D.H., Chard, D.T., Ciccarelli, O., 2012. Clinically isolated syndromes. Lancet Neurology 11 (2), 157–169.
Minagar, A., Toledo, E.G., Alexander, J.S., Kelley, R.E., 2004. Pathogenesis of brain and spinal cord atrophy in multiple sclerosis. J. Neuroimag. Offic. J. Am. Soc. Neuroimag. 14 (3 Suppl), 5s–10s.
Mohammed, H., Hollis, E.R., 2nd, 2018. Cortical reorganization of sensorimotor systems and the role of intracortical circuits after spinal cord injury. 15(3), 588–603.
Noseworthy, J.H., 1994. Clinical scoring methods for multiple sclerosis. Ann. Neurol. (36 Suppl), S80–S85.
Oh, J., Seigo, M., Saidha, S., Sotirchos, E., Zackowski, K., Chen, M., Prince, J., Diener-West, M., Calabresi, P.A., Reich, D.S., 2014. Spinal cord normalization in multiple sclerosis. J. Neuroimag. Offic. J. Am. Soc. Neuroimag. 24 (6), 577–584.
Pardini, M., Yaldizli, O., Sethi, V., Muhlert, N., Liu, Z., Samson, R.S., Altmann, D.R., Ron, M.A., Wheeler-Kingshott, C.A., Miller, D.H., Chard, D.T., 2015. Motor network efficiency and disability in multiple sclerosis. Neurology 85 (13), 1115–1122.
Peterson, R.A., Brown, S.P., 2005. On the use of beta coefficients in meta-analysis. J. Appl. Psychol. 90 (1), 175–181.
Petrova, N., Carassiti, D., Altmann, D.R., Baker, D., Schmierer, K., 2018. Axonal loss in the multiple sclerosis spinal cord revisited. Brain Pathol. 28 (3), 334–348 Zurich, Switzerland.
Rupinski, M.T., Dunlap, W.P., 1996. Approximating Pearson product-moment correlations from Kendall's Tau and Spearman's Rho. Educ. Psychol. Meas. 56 (3), 419–429.
Schlaeger, R., Papinutto, N., Panara, V., Bevan, C., Lobach, I.V., Bucci, M., Caverzasi, E., Gelfand, J.M., Green, A.J., Jordan, K.M., Stern, W.A., von Budingen, H.C., Waubant, E., Zhu, A.H., Goodin, D.S., Cree, B.A., Hauser, S.L., Henry, R.G., 2014. Spinal cord gray matter atrophy correlates with multiple sclerosis disability. Ann. Neurol. 76 (4), 568–580.
Schlaeger, R., Papinutto, N., Zhu, A.H., Lobach, I.V., Bevan, C.J., Bucci, M., Castellano, A., Gelfand, J.M., Graves, J.S., Green, A.J., Jordan, K.M., Keshavan, A., Panara, V., Stern, W.A., von Budingen, H.C., Waubant, E., Goodin, D.S., Cree, B.A., Hauser, S.L., Henry, R.G., 2015. Association between thoracic spinal cord gray matter atrophy and disability in multiple sclerosis. JAMA Neurol. 72 (8), 897–904.
Tsagkas, C., Magon, S., Gaetano, L., Pezold, S., Naegelin, Y., Amann, M., Stippich, C., Cattin, P., Wuerfel, J., Bieri, O., Sprenger, T., Kappos, L., Parmar, K., 2018. Spinal cord volume loss: a marker of disease progression in multiple sclerosis. Neurology 91 (4), e349–e358.
Weeda, M.M., Middelkoop, S.M., Steenwijk, M.D., Daams, M., Amiri, H., Brouwer, I., Killestein, J., Uitdehaag, B.M.J., Dekker, I., Lukas, C., Bellenberg, B., Barkhof, F., Pouwels, P.J.W., Vrenken, H., 2019. Validation of mean upper cervical cord area (MUCCA) measurement techniques in multiple sclerosis (MS): high reproducibility and robustness to lesions, but large software and scanner effects. Neuroimage Clin. 24, 101962.
Xiang, B., Wen, J., Cross, A.H., Yablonskiy, D.A., 2019. Single scan quantitative gradient recalled echo MRI for evaluation of tissue damage in lesions and normal appearing gray and white matter in multiple sclerosis. J. Magnet. Reson. Imag. JMRI 49 (2), 487–498.
Yiannakas, M.C., Mustafa, A.M., De Leener, B., Kearney, H., Tur, C., Altmann, D.R., De Angelis, F., Plantone, D., Ciccarelli, O., Miller, D.H., Cohen-Adad, J., Gandini Wheeler-Kingshott, C.A., 2016. Fully automated segmentation of the cervical cord from T1-weighted MRI using PropSeg: application to multiple sclerosis. Neuroimage Clin. 10, 71–77.
Yousuf, F., Kim, G., Tauhid, S., Glanz, B.I., Chu, R., Tummala, S., Healy, B.C., Bakshi, R., 2016. The contribution of cortical lesions to a composite MRI scale of disease severity in multiple sclerosis. Front. Neurol. 7, 99.